Available online at www.sciencedirect.com
SCIENCE DIRECT®
Polymer 45 (2004) 3643–3650
polymer
www.elsevier.com/locate/polymer

Aggregation behaviour of well defined amphiphilic diblock copolymers with poly(*N*-isopropylacrylamide) and hydrophobic blocks

Markus Nuopponen, Jussi Ojala, Heikki Tenhu*

Laboratory of Polymer Chemistry, Department of Chemistry, University of Helsinki, A.I. Virtasen aukio 1, PB 55, Helsinki FIN-00014 HY, Finland

Received 1 December 2003; received in revised form 23 March 2004; accepted 26 March 2004

Abstract

Series of amphiphilic diblock copolymers with poly(*N*-isopropylacrylamide) as a hydrophilic block and a hydrophobic block consisting of either polystyrene or poly(*tert*-butyl methacrylate) were synthesised using RAFT polymerisations. Differential scanning calorimetry showed the chemically different blocks being phase separated in dry polymers. Light scattering and microcalorimetry studies were performed on aqueous solutions to investigate the phase behavior of the diblock copolymers. By carefully transferring the polymers from an organic solvent to water, either micellar particles or large aggregates were obtained depending on the relative lengths of the blocks. Large aggregates collapsed upon heating, whereas collapse occurred slowly within a broad temperature range in the case of micelle like structures. However, microcalorimetrically the collapse of the PNIPAM chains was observed to take place in all samples, suggesting that the shells of the micellar particles are crowded in a way which hinders the compression of the poly(*N*-isopropylacrylamide) chains.

Keywords: Diblock copolymers; Polymeric micelles; Controlled radical polymerization

1. Introduction

Much effort has recently been focused on the synthesis of tailor-made amphiphilic block copolymers [1–3]. These polymers are interesting for a range of potential applications because of their property to self-assemble into aggregates and micelles when dispersed in selective solvents. Amphiphilic water-soluble polymers can undergo a conformational change in response to an external stimuli [4–6]. The simplest type of aggregation is exhibited by diblock copolymers, which can self-assemble when the hydrophobic core is surrounded by a shell of the solvated hydrophilic part [7,8]. In aqueous solutions, block copolymers with blocks of different hydrophilicities may form random aggregates, micelles, or even more organised structures like, e.g. liposomes. Well-known examples of self-assembling in water are phospholipid cell membranes, surfactants in aqueous solutions, and block copolymers in a way similar to that of surfactants. Self-organisation may also take place in a dry polymer leading to a spontaneous formation of nanoscaled structures due to competing interactions [9]. During the past decades, considerable progress has been made in understanding of the melt phase behavior of block copolymers. Supramolecules self-organise in the form of structure-within-structure morphologies, with a large length scale structure and microphase separation [10,11].

Several syntheses of well-defined block copolymers with predetermined molar masses as well as other polymers with complex molecular architectures have been reported, where the polymers have been prepared using controlled radical polymerisation. Reversible addition-fragmentation chain transfer (RAFT) [12–15] polymerisation is often a method of choice when control on molecular weight and molar mass distribution is needed. RAFT mediated by thiocarbonylthio compounds is an effective and versatile process, applicable to a wide range of vinyl monomers without a need for protecting group. RAFT reactions typically require much less stringent reaction conditions than ionic polymerisation and offer the most of the advantages of conventional free radical polymerisation. With RAFT, the number of easily accessible amphiphilic polymers increase.

Poly(*N*-isopropylacrylamide) [16] (PNIPAM) is one of the most studied thermally responsive polymers. It has a lower critical solution temperature (LCST) around 32 °C in

* Corresponding author. Tel.: +358-9-19150334; fax: +358-9-19150330.
E-mail address: heikki.tenhu@helsinki.fi (H. Tenhu).

0032-3861/$ - see front matter © 2004 Elsevier Ltd. All rights reserved.
doi:10.1016/j.polymer.2004.03.083

water. Above the LCST, the hydrophobic backbone and isopropyl groups of the polymer tend to associate, this causing the collapse of PNIPAM chains, and intra or intermolecular aggregation. However, recent studies have shown that hydrophobic modification or hydrophobic environment affect significantly the behaviour of PNIPAM, leading to new thermoresponsive materials [17–19].

In this work, RAFT polymerisation was utilised to build up series of diblock copolymers comprising of a hydrophilic PNIPAM block and a hydrophobic block, either polystyrene or poly(*tert*-butylmethacrylate). Differential scanning calorimetry (DSC) measurements were performed on dry samples to determine the degree of phase separation [20]. We wanted to study aqueous solutions of the polymers to observe what kind of structures could be formed. Formation of the polymeric nanoparticles with thermally responsive character in water was verified. Thermal properties of polymer aggregates in water were studied by light scattering and microcalorimetry to find out whether PNIPAM behaves independently of the hydrophobes, and whether the particles may be regarded as polymeric micelles. As mentioned above, hydrophobic environment alters the temperature range of dehydration and it has been of interest to find out how would this affect the phase transitions in the case of micelle type particles.

2. Experimental section

2.1. Materials

The monomer *N*-isopropylacrylamide (NIPAM, Polysciences, Ins.) was recrystallised from benzene. Azobis(isobutyronitrile) (AIBN, Fluka) was recrystallised from methanol. Dioxane (Lab-Scan, Analytical Sc.) was distilled before use. Styrene (Aldrich) and *tert*-butylmethacrylate (Aldrich) were distilled under reduced pressure. Benzyl chloride (Aldrich), elemental sulfur, sodium methoxide (Fluka), α-methylstyrene (Aldrich), potassium ferricyanide(III) (Merck), alumina (Merck) and 4,4′-azobis(4-cyanopentanoic acid) (ACPA, Fluka) were used as received. All other solvents with highest purity were used as received.

2.2. Synthesis of 4-cyanopentanoic acid dithiobenzoate (CPADB)

The target compound was prepared by the method of Thang et al. [21]. Dithiobenzoic acid (DTBA) was prepared by the reaction of benzyl chloride (26.3 ml) with elemental sulfur (19.2 g) and sodium methoxide (108 g) in methanol (190 ml) as described elsewhere [15]. DTBA is unstable and was used immediately after preparation. Then, di(thiobenzoyl) disulfide was synthesised. 1.0 N NaOH was added in DTBA (20 mmol) in ether to get sodium dithiobenzoate, which was extracted with water. Potassium ferricyanide(III) (6.59 g, 20 mmol) dissolved in 100 ml water was added dropwise into the aqueous sodium dithiobenzoate solution with stirring. The red precipitate was filtered and the solid was dried in vacuum overnight. The product was recrystallised from ethanol.

Prepared di(thiobenzoyl) disulfide (1.5 g, 5.1 mmol), dry 4,4′-azobis(4-cyanopentanoic acid) (2.2 g, 7.9 mmol) and distilled ethyl acetate (30.0 ml) were added in to a round-bottomed flask and the solution was heated at reflux (85 °C) for 19 h. Ethyl acetate was removed in vacuum. The crude product was isolated by column chromatography (silicagel 60 Å) using ethyl acetate–hexane (2:3) as eluent. Red fractions were collected and the solvent mixture was removed under vacuum. Red residue was placed in a freezer to crystallise. The product was recrystallised from benzene. ^{1}H NMR ($CDCl_3$) [200 MHz] ppm: 1.95 (3H); 2.30–2.75 (4H); 7.40–7.85 (5H) (Scheme 1).

2.3. Polymerisations

2.3.1. Preparation of polystyrene

Styrene (5 ml), CPADB (26 mg) and AIBN (1.5 mg) were dissolved in 1,4-dioxane 15 ml. The other polymerisation was conducted in bulk, where CPADB (46 mg) and AIBN (4,0 mg) were dissolved in styrene (10 ml). Solutions were degassed by three freeze-pump-thaw cycles. Vessel were sealed under vacuum and placed in a thermostatically controlled oil bath (60 °C) for 42 and 23 h. After the polymerisation the reaction mixture was dissolved in THF, the polymer was precipitated in cold methanol and purified by repeated precipitations. Product was dried in vacuum.

2.3.2. Preparation of poly(tert-butylmethacrylate)

A solution of *t*-BMA (5.0 ml), CPADB (36.6 mg) and AIBN (2.2 mg) in 1,4-dioxane (5.6 ml) was added to a reaction vessel. System was degassed by three freeze-pump-thaw cycles, sealed under vacuum and placed in a thermostated oil bath (70 °C) for 46 h. The polymer was precipitated in a water–methanol mixture (1:4) and separated by centrifugation. Precipitation was repeated twice and the product was dried under vacuum.

2.3.3. Preparation of poly(N-isopropylacrylamide-block-styrenes)

Well characterised homopolymers synthesised at the first step were used as macro RAFT agents. PS (1.0 g, 8000 g mol^{-1}) was dissolved in 1,4-dioxane (20 ml) before adding NIPAM (4.2 g) and AIBN (2.2 mg). The other PS (0.35 g, 5200 g mol^{-1}), NIPAM (3.2 g) and AIBN (1.5 g) were dissolved in 1,4-dioxane (15 ml) as well. The systems

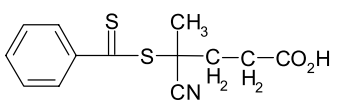

Scheme 1. 4-Cyanopentanoic acid dithiobenzoate.

were degassed by three freeze-pump-thaw cycles, sealed under vacuum and placed in a thermostated oil bath (60 °C) for 42 h. The polymers were precipitated in diethyl ether, conversions being around 40 and 60%. Volatile materials were removed in vacuum to yield pink powders (Scheme 2).

2.3.4. Preparation of poly(N-isopropylacrylamide-block-tert-butylmethacrylates)

Well characterised P(*t*-BMA) RAFT macroinitiator (1.15 g) was dissolved in 1,4-dioxane (10.5 ml) before adding NIPAM (3.3 g) monomers and AIBN (1,6 mg). The system was degassed by three freeze-pump-thaw cycles, sealed under vacuum and placed in a thermostated oil bath (70 °C) for 44 h. The polymers were precipitated in water/methanol (1:1) mixture and conversions in reactions was around 30%. Purification was repeated by dissolving polymer in chloroform and precipitating in water/methanol.

2.4. Micelle formation

Diblock copolymers were dissolved in *N*,*N*-dimethylacetamide (DMA, 0.5 wt%), which is a common solvent for all blocks. Deionised water was added dropwise to the solutions with vigorous stirring. 15–25 wt% of water was added depending on polymer. The quality of the solvent became gradually poorer for the hydrophobic blocks, this causing the aggregation of the hydrophobic blocks observed as the turbidity of the solutions. The resulting slightly opaque solutions were placed in dialysis bags (Cellu Sep T1, nominal MWCO:3500) and dialysed against purified water to remove DMA.

2.5. Instrumentation and characterisation

2.5.1. Size exclusion chromatography (SEC)

The molar masses (M_n) and molar mass distributions (M_w/M_n) were determined using Waters SEC equipment with Styragel columns, a Waters 2410 refractive index detector and Waters 2487 UV detector. THF was used as an eluent, flow rate being 0.8 ml/min and the calibration was carried out with polystyrene standards (Showa Denko).

2.5.2. Light scattering

DLS measurements were conducted with a Brookhaven Instruments BI-200 SM goniometer and a BI-9000 AT digital correlator. Light source was a Lexel 85 Argon laser (514.5 nm power range of 15–150 mW) except in static light scattering (SLS) studies where the wavelength of the laser was 632.8 nm. Time correlation functions were analysed with a Laplace inversion program CONTIN. Hydrodynamic radii (R_h) of the aggregates were measured using DLS at 20, 30, 40 and 50 °C. Solutions ($c_p = 0.1 \times$ mg/ml) were equilibrated for 30 min before the measurements. In the DLS the intensity–intensity time correlation function $G^2(t)$ was determined, which was used for the determination of the average line width (Γ). The average translational diffusion coefficient $\langle D \rangle$ was further calculated from (Γ/q^2). Stokes–Einstein equation was used to determine the hydrodynamic radii $k_B T/(6\pi\eta\langle D\rangle$ with k_B, η, T being Boltzmann constant, the solvent viscosity and absolute temperature, respectively.

Radius of gyration, R_g, was also determined by SLS. Scattering intensity, where the effect of solvent and scattering angle has been taken into consideration can be written as $I_\theta = (I_{\theta,\text{solution}} - I_{\theta,\text{solvent}})\sin\theta$, with $I_{\theta,\text{solution}}$, $I_{\theta,\text{solvent}}$, θ being the scattering intensity of the solution, scattering intensity of the solvent and scattering angle, respectively. I_θ has been presented as a function of q^2. Scattering function $P(q)$ is written as $P(q) = I_\theta/I_{\theta=0} = 1 - ((R_g^2 q^2)/3)$ where $I_{\theta=0}$ is the estimated extrapolated intensity at zero angle. Thus, $q = (4\pi n_0/\lambda)(\sin(\theta/2))$ is the scattering vector with n_0 and λ are refractive index of solvent and wavelength. It is essential to use the linear part of the scattering function where R_g is proportional its slope, i.e. $q\langle R_g\rangle \leq 1$. This linear part can be estimated using R_h values determined before.

SLS was used to determine the weight-average molar mass (M_w) of the aggregates at 20, 30, 40 and 50 °C. Equipment was calibrated using toluene ($T = 20$ °C, $\theta = 90°$ and $\lambda = 632.8$ nm). The SLS data were treated using a Zimm's double extrapolation method. Concentrations of the polymer solutions varied between 5×10^{-3}–1×10^{-1} mg/ml. The average radius of gyration $\langle R_g\rangle$ was determined as well.

2.5.3. The specific refractive index increment measurements

The specific refractive index increment (d*n*/d*c*) values were determined with Cromatix KMX-16 laser differential refractometer. Light source was helium–neon laser (632.8 nm). d*n*/d*c* values of the block copolymers were measured for constant K which includes d*n*/d*c*. $K = (4\pi^2 n_0^2/\lambda^4 N_A)(\text{d}n/\text{d}c)^2$ with N_A, n_0 and λ_0 being Avogadro's constant, the solvent refractive index and the wavelength of the light, respectively. A series of five solutions with different concentrations (0.6–2.3 mg/ml) was prepared. d*n*/d*c* values for the solutions were measured 20, 30 and 40 °C. The average of different solutions at each temperature was used in the calculation of M_w.

2.5.4. Nuclear magnetic resonance spectroscopy

^{1}H NMR spectra of the polymers were measured at ambient temperature with a 200 MHz Varian Gemini 2000 spectrometer using deuterated chloroform as a solvent.

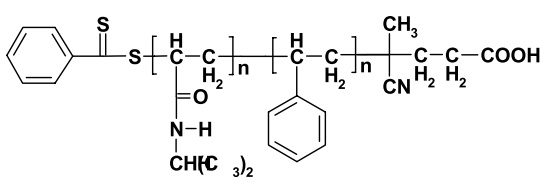

Scheme 2. Poly(*N*-isopropylacrylamide)-block-polystyrene.

2.5.5. Differential scanning calorimetry

DSC measurements on dry polymer samples were performed with a Mettler Toledo DSC822. The samples were heated from 20 to 180 °C (2 or 10 °C min^{-1}), then cooled down to 20 °C (10 °C min^{-1}) and reheated to 180 °C (2 or 10 °C min^{-1}). Several measurements were performed for each sample.

2.5.6. Microcalorimetry

Thermal transitions of dilute aqueous solutions of both PS and P(*t*-BMA) containing polymers were measured with a Microcal VP-DSC. Temperature interval was from 5 to 65 °C and heating rates varied from 0.5 to 1.5 °C min^{-1}.

2.5.7. Cryo-electron microscopy

Samples were prepared by vitrification in liquid ethane. Gatan CT 3500 cryostage was used to observe the sample on FEI Tecnai F20 electron microscope at 200 kV under low dose conditions. Electron micrographs were recorded on Kodak SO-163 film at nominal magnification of 62,000 ×.

3. Results and discussion

3.1. Synthesis and characterisation of homo and diblock polymers

Dithioesters are effective chain transfers agents (CTA) often used in RAFT reactions [13]. CPADB was selected for a RAFT agent as it has turned out to be effective in certain polymerisations [22] and carboxylic acid facilitates the further functionalisation of the polymer. Syntheses of the homopolymers are described in Table 1. Polymerisations fulfilled one criterion of controlled polymerisations as the number-average molar masses (M_n) obtained by SEC were usually in a good agreement with the values estimated theoretically. Theoretical values were calculated based on the polymer yields, assuming that the RAFT agent was totally reacted. The number average molar masses are calculated using the equation: $M_{n,theor} = [M] \times MW_{mon} \times conv/[CTA] + MW_{CTA}$, where [M], MW_{mon}, conv, [CTA] and MW_{CTA} are the initial concentration of the monomer, molar mass of the monomer, fraction conversion, initial concentration of the RAFT agent and the molar mass of the RAFT agent, respectively.

In the next stage, near-monodisperse PS and P(*t*-BMA) polymers were used as macro RAFT agents in the syntheses of block polymers. As a result, well-defined diblock copolymers of PNIPAM-*b*-PS/P(*t*-BMA) with an appropriate hydrophilic/hydrophobic balance were successfully prepared, as is shown in Table 2. The growth of the block copolymers was confirmed by SEC and spectroscopic analysis using ^{1}H NMR. However, SEC results for the block polymers with PNIPAM blocks are assumed to be somewhat inaccurate, because of some difficulties due to PNIPAM character in SEC measurements [23,24]. Thus, the M_n of the block polymers were calculated from the intensities of the characteristic peaks in ^{1}H NMR, using the data obtained with the homopolymers.

3.2. DSC measurements

The glass transition temperatures of dry polymers were measured to get an estimate of the possible mixing of the chemically different blocks. The glass transition temperatures of synthesised copolymers are collected in Table 3. The results show that different blocks are phase separated while there are two separate T_gs similar to the corresponding pure homopolymer segments. In addition, the block ratio of the segments and molar mass do not affect the T_gs. In the case of mixtures of compatible polymers the glass transition temperatures should change with changing volume ratios of the polymers. In the present case, T_g of polystyrene is higher in the block copolymers compared to that of pure PS, due to restrictions by PNIPAM. When considering the compatibilities of chemically different amorphous polymers, ΔC_p associated with the glass transition may be used to evaluate the degree of mixing. In the present case, within the experimental error, the chemically different blocks are strongly phase separated. This observation is as expected in the case of block copolymers containing PS blocks. Methacrylate blocks in spite of their higher polarity compared to polystyrene, phase separate as well.

3.3. Micelle formation

The capability of the diblock copolymers to build up micellar structures was studied by carefully transferring the polymers from an organic solvent into aqueous solution. It should be noted that all the three polymers used in these

Table 1
Syntheses and characteristics of homopolymers

Monomer A (concentration, solvent, temperature)	CTA[a] (mM)	AIBN (mM)	Conversion[b] (%)	$M_{n,theo}$ (g mol^{-1})	M_n[c] (g mol^{-1})	M_w/M_n[c]
Styrene (bulk, 60 °C)	16.5	2.43	14	8000	8000	1.05
Styrene (2.9 M, dioxane, 60 °C)	4.7	0.46	8	3900	5200	1.08
t-BMA(6.0 M, dioxane, 70 °C)	12.3	1.26	39	15,100	19,400	1.15

[a] Chain transfer agent 4-cyanopentanoic acid dithiobenzoate.
[b] As determined gravimetrically.
[c] Determined by SEC using calibration with PS standards.

Table 2
Syntheses and characteristics of block polymers

Polymer, monomer B (concentration, temperature)[a]	Block A[b] (CTA, M_n, concentration)[c]	$M_{n,theo}$ (g mol^{-1})	M_n[d] (g mol^{-1})	M_w/M_n[e]	PNIPAM mol%[f]
A NIPAM (1.9 M, 60 °C)	PS (5200, 4.5 mM)	33,900	44,300	1.34	88
B NIPAM (1.9 M, 60 °C)	PS (8000, 6.3 mM)	21,700	21,600	1.15	62
C NIPAM (2.7 M, 70 °C)	*t*-BMA (19400, 5.6 mM)	35,800	33,300	1.13	47

[a] Polymerisations were conducted in 1,4-dioxane.
[b] RAFT macro transfer agent (g mol^{-1}).
[c] Chain transfer agent 4-cyanopentanoic acid dithiobenzoate.
[d] M_n of the A–B block copolymer determined with ^{1}H NMR spectroscopy.
[e] Determined by SEC using calibration with PS standards.
[f] Determined with ^{1}H NMR spectroscopy.

experiments have a carboxylic end group in the hydrophobic block. It may be assumed that in the non-polar core of the particles the acid groups do not dissociate [25] but tend to form hydrogen bonds, this promoting the build up of core-shell structures.

3.4. Light scattering

Three samples were studied and the hydrodynamic sizes of the particles were measured by dynamic light scattering at 20, 30, 40 and 50 °C. As is shown in Fig. 1, the diameters of the particles formed by the polymers vary between 60 and 600 nm at room temperature. So, it is evident that the polymers form different structures in water. The aggregation process depends on the hydrophobicity of the block copolymers. Polymer A forms large aggregates, diameter at room temperature being around 600 nm, most probably due to the long hydrophilic PNIPAM block which disrupts the micelle formation. It may be assumed that this polymer builds up non-structured aggregates where the hydrophilic chains are interconnected by the associations of the hydrophobic blocks. Two other polymers (B and C) form much smaller structures due to shorter PNIPAM blocks. A more fundamental difference between the three samples is observed when they are heated up to 50 °C (Fig. 2). The large aggregates collapse, and the diameter decrease to 200 nm. Under the same conditions, particles formed by the polymers B and C do not seem to shrink considerably upon heating. It may be assumed that the hydrophobic blocks are long enough to form a dense core and thus, to force PNIPAM to organise as a particle shell. The core-shell structures keep the aggregates stabile and reduce the degree of shrinking noticeably when temperature is increased. An interesting observation is that the intensity of the scattered light is time independent, which indicates that particles are stable, as intensity is very sensitive to the aggregation. That is to say, these particles are colloidally stable, the precipitation at elevated temperature does not occur even upon prolonged heating at 50 °C for several days.

SLS was used to determine the radii of gyration, $\langle R_g \rangle$ [26]. Typical angular dependence of the reciprocal scattering function is shown for sample B in Fig. 3. $\langle R_g \rangle$ is calculated from the linear part of the function as described in the experimental part. In Fig. 4, a typical Zimm plot for one of the samples. Values of $\langle R_g \rangle / \langle R_h \rangle$ were examined to get information about the shape of the aggregates [27]. The polydispersity of the aggregates may reduce the significance of the ratio $\langle R_g \rangle / \langle R_h \rangle$, but some general conclusions may be drawn, however. Aggregates of B and C, the more hydrophobic polymers, have generally values of $\langle R_g \rangle / \langle R_h \rangle$ greater than 1 after the dehydration process at elevated temperatures, this indicating a final shape of loose spheres. Polymer C forms particles with a very high aggregation number (see below), and the $\langle R_g \rangle / \langle R_h \rangle$ is constant irrespective of temperature. On the other hand, the scattering intensity from sample A increases considerably above the LCST of PNIPAM. We suppose that the large polymer aggregates do not keep a stabile form, but aggregate together simultaneously as the PNIPAM chains collapse.

The aggregation number and the radii of the micellar particles (B and C) as functions of the degree of polymerisation are indicative of crew-cut micelles [28]. The aggregation numbers of the micelles were estimated using the known values of N_A and N_B, with the scaling

Table 3
Glass transition temperatures by DSC

Polymer	PNIPAM mol%[a]	M_n PNIPAM (g mol^{-1})	M_n PS or P(*t*-BMA) (g mol^{-1})	M_w/M_n	T_{g1} (°C)[b]	T_{g2} (°C)[c]
A PS-*b*-PNIPAM	88	39,100	5200	1.34	106.0	137.1
B PS-*b*-PNIPAM	62	13,600	8000	1.15	107.3	133.3
C P(*t*-BMA)-PNIPAM	47	13,900	19,400	1.13	118.1	134.3

[a] Composition based on ^{1}H NMR.
[b] T_g of the hydrophobic block.
[c] T_g of the PNIPAM block.

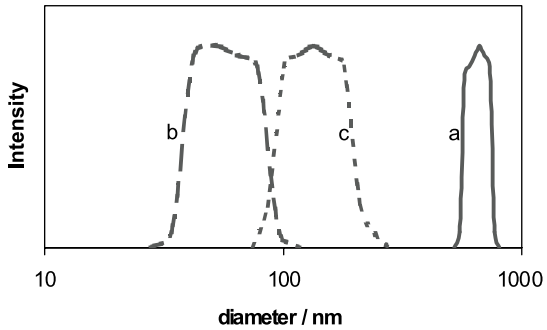

Fig. 1. Size distributions of the aggregates at 20 °C. Polymer concentration 0.2 g/l. For a, b, c, see Table 2.

relation by Förster et al. $Z = N_A^{\alpha} N_B^{-\beta}$, where Z is the aggregation number, N_A and N_B are the degree of polymerisation of the A and B blocks, and α and β are fitting parameters. Values obtained for PS containing aggregates are well in accordance with the measured ones. However, the value of the Z calculated for the polymer with a P(*t*-BMA) block deviates considerably from the experimental value, this probably indicating raspberry like shape of P(*t*-BMA) aggregates, which consist of several smaller spherical particles. This is visualised in electron micrograph (Fig. 5). Where as, crew-cut micelles of polymer B remain separated due to larger PNIPAM content.

We were also interested to know the number of polymers in the aggregates as a function of temperature even though it is assumed to remain stable due to the glassy state of their cores [29]. The aggregation numbers were evaluated by SLS (Table 4). The main observation here is that the aggregation number changes only slightly with temperature, except in the case of unstable particle A. In this case particle scattering increased hugely and the aggregation number could not be measured. Again, it may be concluded that the stable particles (B and C) retain their form upon heating in a way that the interactions of the PNIPAM shells do not increase and the particles do not aggregate in dilute samples. Note the LS measurements were conducted only up to 40 °C because the d*n*/d*c* could not be determined at higher temperatures. The fact that the particle sizes in samples B and C change slowly upon heating indicates that there is not enough space around the small hydrophobic core to allow

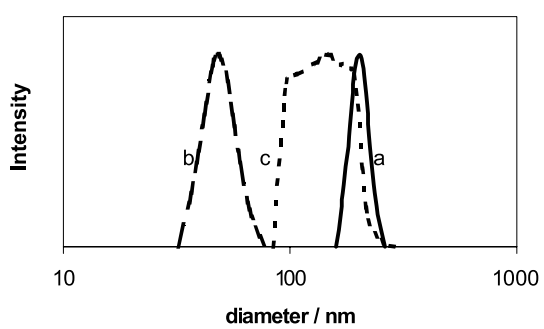

Fig. 2. Size distributions of the aggregates at 50 °C. Polymer concentration 0.2 g/l. For a, b, c, see Table 2.

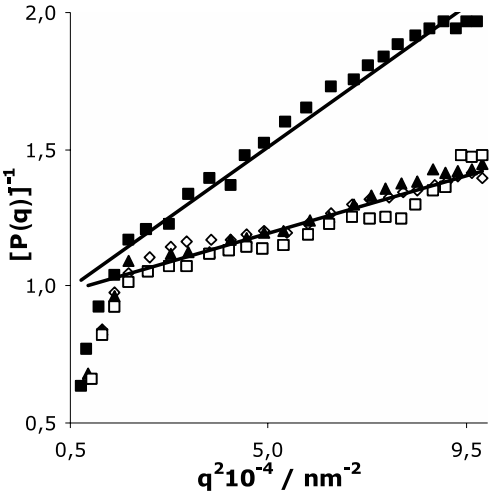

Fig. 3. Angular dependences of $\{P(q)\}^{-1}$ of polymer B at different temperatures, 20 (■), 30 (◇), 40 (□) and 50 (▲) °C. Polymer concentration 0.1 mg/ml. R_g decreases as temperature increases over the LCST of the polymer.

the PNIPAM chains to contract onto the surface of the nucleus. The estimated footprint per PNIPAM chain on the core surface is of the order of 5 nm^2 and does not change with temperature. This conclusion, in fact, is somewhat similar to the recent observations by Hu et al. [17] on thermally responsive polymer particles grafted with PNIPAM chains.

3.5. Microcalorimetric measurements

Samples studied by DLS were also measured in a microcalorimeter. Some thermograms are shown in Fig. 6. All three samples (A, B and C) showed ΔH values within the same range (around 20–30 J/g PNIPAM) even though the enthalpy change was somewhat smaller for *t*-BMA polymer compared to PS polymers. Polymer A showed an onset temperature typical to pure PNIPAM, whereas the other two polymers, much more hydrophobic, started to dehydrate at noticeably lower temperatures, thus, hydrophobic blocks lowered the maximum temperature of the dehydration of the PNIPAM brushes, as is expected. Also, the temperature range of the PNIPAM collapse broadened

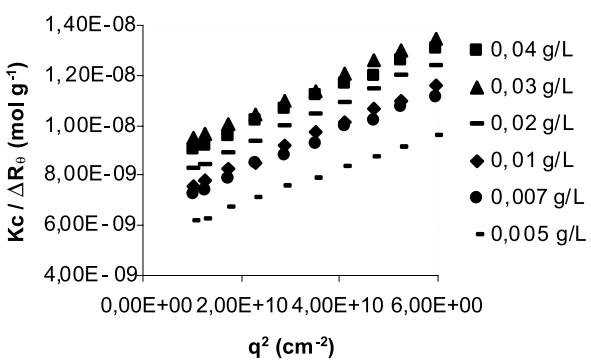

Fig. 4. A typical Zimm plot of polymer C at 20 °C.

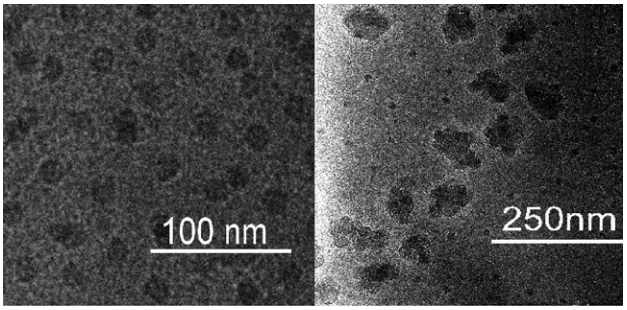

Fig. 5. Cryo-electron microscopy images of aggregate B (left) and C (right).

as the size of the hydrophobe increased in the aggregate core. The dehydration took place over a temperature range ~15–40 °C. It has been shown that PNIPAM dehydrates slowly due to the stabile structures of the micellar particles. For the same reason the dehydration does not necessarily lead to a huge change in the particle size. This may be rationalised by concluding that polymer A has the highest PNIPAM content, evidently high enough to disturb the formation of a micelle with a hydrophobic core. Samples B and C, on the other hand, form micelles with dimensions of the same order of magnitude as the dimensions of the fully stretched macromolecules.

4. Conclusions

Amphiphilic diblock copolymers with low polydispersities have been successfully synthesised using RAFT reactions. PNIPAM has been used as a hydrophilic block, and either PS or P(*t*-BMA) as the hydrophobe. The mutual lengths of the blocks have been varied. According to DSC, the chemically different blocks are strongly segregated in dry polymers. In water, the copolymers with hydrophobic blocks long enough form micellar particles. When the length of the PNIPAM block is increased, large aggregates instead of micelles form up. The large aggregates collapse upon heating, whereas the change in the particle size is modest and very gradual in the case of the micelles. Microcalorimetrically it has been shown that the dehydration of the PNIPAM chains takes place in all samples, but with the micellar structures, the change takes place within a broad temperature range. It is concluded that the surface of the hydrophobic core of the small particles is crowded in a way that hinders the compression of the PNIPAM shell. Surprisingly, the micellar particles were observed to be colloidally stable, and they did not precipitate from water at elevated temperatures. This finding will be subject to further studies.

Table 4
Light scattering data on polymer aggregates

Sample[a]	Temperature (°C)	$M_{w,aggregate}$[b] (10^6 g mol^{-1})	N_{polym}[c]	$\langle R_h \rangle$ (nm)	$\langle R_g \rangle$[d] (nm)	$\langle R_g \rangle / \langle R_h \rangle$
A	20	167	2813	300	265	0.88
	30	184	3099	250	223	0.89
	40[e]	–	–	120	155	1.29
B	20	10.1	407	38	55	1.46
	30	12.0	483	32	35	1.11
	40	15.0	602	33	37	1.12
C	20	164	4358	61	68	1.13
	30	162	4305	58	65	1.12
	40	184	4890	55	65	1.18

[a] Polymers described in Table 3.
[b] Measured with SLS.
[c] Aggregation number, $M_{w,aggregate}/M_{w,polymer}$.
[d] Measured with DLS.
[e] Zimm plot could not be measured at 40 °C.

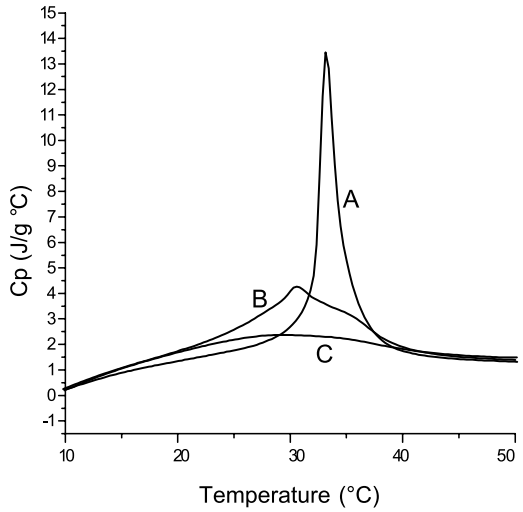

Fig. 6. Thermograms of aqueous solutions, heating rate 1 °C min^{-1}. PNIPAM concentrations in solutions a, b and c: 0.88, 0.63 and 0.47 g/l.

Acknowledgements

The work was supported by the Finnish Technology Agency (TEKES) and INTAS (INTAS-01-607). We are grateful to P. Laurinmäki and S. Butcher, Electron Microscopy unit of the Institute of Biotechnology, University of Helsinki, for electron microscopy images.

References

[1] Chong YK, Le TPT, Moad G, Rizzardo E, Thang SH. Macromolecules 1999;32:2071.
[2] Zhang L, Eisenberg A. J Am Chem Soc 1996;118:3168.
[3] Luo L, Eisenberg A. Langmuir 2001;17:6804.
[4] Virtanen J, Tenhu H. Macromolecules 2000;33:5970.
[5] Arotcarena M, Heise B, Ishaya S, Laschewsky A. J Am Chem Soc 2002;124:3787.
[6] Virtanen J, Arotcarena M, Heise B, Ishaya S, Laschewsky A, Tenhu H. Langmuir 2002;18:5360.
[7] Chung JE, Yokoyama M, Okano T. J Control Release 2000;65:93.
[8] Virtanen J, Holappa S, Lemmetyinen H, Tenhu H. Macromolecules 2002;35:4763.

[9] Mäki-Ontto R, de Moel K, de Odorico W, Ruokolainen J, Stamm M, ten Brinke G, Ikkala O. Adv Mat 2001;13:117.
[10] Ikkala O, ten Brinke G. Science 2002;295:2407.
[11] Klok HA, Lecommandoux S. Adv Mat 2001;13:1217.
[12] Chiefari J, Chong YK, Ercole F, Krstina J, Jeffery J, Le TPT, Mayadunne RTA, Meijs GF, Moad CL, Moad G, Rizzardo E, Thang SH. Macromolecules 1998;31:5559.
[13] Le TP, Moad G, Rizzardo E, Thang SH. PCT Int Appl WO 9801478 A1 980115.
[14] Moad G, Chiefari J, Chong YK, Krstina J, Mayadunne RTA, Postma A, Rizzardo E, Thang SH. Polym Int 2000;49:993.
[15] Mitsukami Y, Donovan MS, Lowe AB, McCormick CL. Macromolecules 2001;34:2248.
[16] Schild HG. Prog Polym Sci 1992;17:163.
[17] Hu T, You Y, Pan C, Wu C. J Phys Chem B 2002;106:6659.
[18] Balamurugan S, Mendez S, Balamurugan SS, O'Brien II MJ, Lopez GP. Langmuir 2003;19:2545.
[19] Nichifor M, Zhu XX. Polymer 2003;44:3053.
[20] Garcia MF, de la Fuente JL, Fernandez-Sanz M, Madruga EL. Polymer 2001;42:9405.
[21] Thang SH, Chong YK, Mayadunne RTA, Moad G, Rizzardo E. Tetrahedron Lett 1999;40:2435.
[22] Chong YK, Krstina J, Le TPT, Moad G, Postma A, Rizzardo E, Thang SH. Macromolecules 2003;36:2256.
[23] Ganachaud F, Monteiro MJ, Gilbert RG, Dourges MA, Thang SH, Rizzardo E. Macromolecules 2000;33:6738.
[24] Schilli C, Lanzendorfer MG, Muller AHE. Macromolecules 2002;35:6819.
[25] Khokhlov A, Kramarenko AY. Macromolecules 1996;29:681.
[26] Harding SE, Sattelle DB, Bloomfield VA. Laser light scattering in biochemistry. Cambridge: The Royal Society of Chemistry; 1992.
[27] Burchard W, Schmidt M, Stockmayer WH. Macromolecules 1980;13:1265.
[28] Förster S, Zisenis M, Wenz E, Antonietti M. J Chem Phys 1996;104:9956.
[29] Stepanek M, Podhajecka K, Tesarova E, Prochazka K. Langmuir 2001;17:4240.